New caged neurotransmitter analogs selective for glutamate receptor sub-types based on methoxynitroindoline and nitrophenylethoxycarbonyl caging groups

Francisco Palma-Cerda, Céline Auger, Duncan J Crawford, Andrew C.C. Hodgson, Stephen J Reynolds, Justin K Cowell, Karl A.D. Swift, Ondrej Cais, Ladislav Vyklicky, John E.T. Corrie, et al.

New caged neurotransmitter analogs selective for glutamate receptor subtypes based on methoxynitroindoline and nitrophenylethoxycarbonyl caging groups

Francisco Palma-Cerda a, Céline Auger a, Duncan J. Crawford b, Andrew C.C. Hodgson b, Stephen J. Reynolds b, Justin K. Cowell b, Karl A.D. Swift b, Ondrej Cais c, Ladislav Vyklicky c, John E.T. Corrie d, David Ogden a,*

a Université Paris Descartes, 75006 Paris, France
b Tocris Bioscience, Bristol BS11 0QL, United Kingdom
c Institute of Physiology ASCR, CZ-14220 Prague, Czech Republic
d MRC National Institute for Medical Research, London NW7 1AA, United Kingdom

Abstract

Photolysis is widely used in experimental neuroscience to isolate post-synaptic receptor activation from presynaptic processes, to determine receptor mechanisms in situ, for pharmacological dissection of signaling pathways, or for photostimulation/inhibition in neural networks. We have evaluated new caged neuroactive amino acids that use 4-methoxy-7-nitroindolinyl- (MNI) or 1-(2-nitrophenyl)ethoxycarbonyl (NPEC) photoprotecting groups to make caged ligands specific for glutamate receptor subtypes. Each was tested for interference with synaptic transmission and excitability and for receptor specific actions in slice preparations. No adverse effects were found at glutamate receptors. At high concentration, MNI-caged, but not NPEC-caged ligands, interfered with GABA-ergic transmission.

MNI-caged amino acids have sub-microsecond release times suitable for investigating mechanisms at fast synaptic receptors in situ. MNI-NMDA and MNI-kainate were synthesized and tested. MNI-NMDA showed stoichiometric release of chirally pure NMDA. Wide-field photolysis in cerebellar interneurons produced a fast-rising sustained activation of NMDA receptors, and localized laser photolysis gave a fast, transient response. Photolysis of MNI-kainate to release up to 4 μM kainate generated large inward currents at resting membrane potential in Purkinje neurons. Application of GYKI 53655 indicated that 40% of the current was due to AMPA receptor activation by kainate. Signaling via metabotropic glutamate receptors (mGluR) does not require fast release rates. NPEC cages are simpler to prepare but have slower photorelease. Photolysis of NPEC-ACPD or NPEC-DHPG in Purkinje neurons generated slow inward currents blocked by the mGluRtype1 antagonist CPCCOEt similar to the slow sEPSC seen with parallel fiber burst stimulation. NPEC-AMPA was also tested in Purkinje neurons and showed large sustained inward currents selective for AMPA receptors with little activation of kainate receptors. MNI-caged L-glutamate, NMDA and kainate inhibit GABA-A receptors with IC50 concentrations close to the maximum concentrations useful in receptor signaling experiments.

Keywords: Caged neurotransmitters, Glutamate receptors, Ionotropic receptors, Metabotropic receptors

1- Introduction

Flash photolysis of inert photolabile precursors -'caged' ligands- is an experimental tool that enables the release of ligands adjacent to their receptors to overcome slow diffusion in the extracellular or intracellular compartments that would otherwise determine the rates of receptor activation. Photolysis allows diffusional equilibration of the caged ligand in the extracellular or intracellular space adjacent to receptors before photorelease by a pulse of light from a laser, flashlamp or LED source. This is usually at near-UV wavelengths and combined with conventional or laser scanning microscopy. The ligands can be applied on the same timescales and with similar spatial scales as in their physiological context. The method is used in neuroscience to activate receptors at synapses in situ in brain slices, and intracellularly to study second messenger signaling pathways. Detailed kinetic investigations can be made of receptor mechanisms (Canepari and Ogden, 2006; DiGregorio et al., 2007) and intracellular signaling pathways (Khodakhah and Ogden, 1995). It can also be used to apply labile transmitters such as nitric oxide, cannabinoids or ATP (Murphy et al., 1994; Jabs et al., 2007; Heinbockel et al., 2005) at known concentration, minimizing effects of catabolism or uptake on the concentration reaching the receptors.

The application of photolysis in neuroscience depends mainly on the availability of caged ligands with suitable photochemical and pharmacological properties but the design, synthesis and testing of caged neurotransmitters and other caged receptor ligands has generally slowed the introduction of new reagents. Here we have applied photochemistry that is well-established in this field to generate caged ligands showing specificity for glutamate receptor sub-types. A significant issue in developing photolabile precursors of neuroactive amino acids has been their level of stability to hydrolysis. Reagents with poor resistance to hydrolysis can leak active neurotransmitter during equilibration with the biological preparation, causing receptor desensitization. 7-Nitroindolinyl- and 4-methoxy-7-nitroindolinyl-L-glutamate were introduced as reagents with good hydrolytic stability (Papageorgiou et al., 1999; Papageorgiou and Corrie, 2000) and have fast, sub-microsecond timescale photolysis reactions (Morrison et al., 2002). They have been widely used since in kinetic investigations of glutamate receptors and for photostimulation (for example Canepari et al., 2001a,b; Matsuzaki et al., 2001; Gasparini and Magee, 2006; DiGregorio et al., 2007; Trigo et al., 2009a). This approach has been adapted here to generate the receptor-specific caged ligands MNI-NMDA and MNI-kainate. For other glutamate receptor ligands we have used 2-nitrobenzyl-based photochemistry to produce stable protection of amino groups (Corrie et al., 1993). These NPEC-caged ligands have slower release rates upon photolysis, on a 50-100 ms timescale, and are suitable for studying G-protein coupled metabotropic receptor signaling. Here we report tests of the new reagents for use as experimental tools in neuroscience.

1.1. Photochemistry of NPEC- and MNI-caged ligands

Synthesis of the new caged ligands was based on published protocols for MNI- and NPEC-caged L-glutamate (Papageorgiou and Corrie, 2000, 2002) and (Corrie et al., 1993) respectively. Structures of the new compounds and outlines of the photochemical cleavage reactions are shown in Fig. 1. Spectroscopic data that verify the structures are given in Supplementary information.

NPEC-caged L-glutamate (N-1-(2-nitrophenyl)ethoxycarbonyl-L-glutamate) was introduced as an efficient caged L-glutamate that is resistant to hydrolysis. The synthesis, photochemical properties, mechanistic investigations and application as a caged neurotransmitter at the squid giant synapse were described by Corrie et al. (1993). The synthesis was adapted here to generate NPEC-ACDP, NPEC-DHPG and NPEC-AMPA (Fig. 1). The NPEC caging group has been shown to be efficient with near-UV photolysis: the extinction coefficient (ε347 660 M^{-1} cm^{-1}) and quantum yield (Q_P 0.63; Corrie et al., 1993) were similar to those of the well-characterized caged ATP, the P^3-1-(2-nitrophenyl)ethyl ester of ATP (Walker et al.,1988). However the NPEC-caged amino acids have the disadvantage that after light absorption the rate of release of ligands at physiological pH

is slow, approximately 10 s^{-1} (Corrie et al., 1993). They are thus less suitable for kinetic studies of fast synaptic receptors in mammalian preparations because the photolysis reaction would be rate-limiting for activation, but may be useful in investigation of slower processes such as desensitization and trafficking. In contrast, the kinetics of metabotropic glutamate receptor signaling are on a 100 ms timescale (Canepari and Ogden, 2006) so NPEC-caged ligands can be used in this context. Although the NPEC-caged ligands are efficient in one-photon near-UV photolysis, the two-photon efficiency of nitrophenyl caged reagents is too small to be useful (photolysis two-photon cross-section <0.01 GM; Brown et al., 1999).

The nitroindoline and methoxynitroindoline (MNI; 4-methoxy- 7-nitroindoline) caging groups were developed for photolysis in aqueous solution (Papageorgiou et al., 1999; Papageorgiou and Corrie, 2000, 2002). MNI-caged L-glutamate has been widely used in neuroscience. The nitroindolines are stable to hydrolysis at physiological pH and efficient for one-photon near-UV excitation without apparent toxicity (Canepari et al., 2001a). The release rate after light absorption is fast compared with ionotropic glutamate receptor activation (5 X 10^6 s^{-1}; Morrison et al., 2002). Neither Ninor MNI-caged L-glutamate interferes with glutamate receptors at concentrations up to 10 mM.

Although efficient in one-photon absorption, the MNI-caged amino acids have poor efficiency in two-photon photolysis, the photolysis cross-section has been measured as 0.02-0.06 GM at 720 nm (Matsuzaki et al., 2001; D.O. unpublished data). This is about 1000-fold less efficient than one-photon absorption in the near-UV. Thus, releasing sufficient glutamate to activate postsynaptic receptors with good localization by two-photon photolysis of MNI-L-glutamate requires high cage concentrations and high light intensities. One reason for the use of two-photon near-IR excitation is to avoid the problem of light absorption by the cage between water-dipping objectives and cell that prevents the efficient transmission of near-UV light to the preparation. However this 'inner filtering' effect of the cage can be overcome more easily by excitation away from the peak for one-photon absorption with a 405 nm diode laser. This gives efficient, localized, one-photon photolysis in a sub-micron spot with MNI-caged ligands present at mM concentration in the bath solution (Trigo et al., 2009a).

2. Methods

2.1. Slice preparation

Experiments were made with parasagittal slices 200 μm thick cut from the cerebellum of Sprague Dawley rats, age 18-21 days for recordings from Purkinje neurons or 12-16 days for molecular layer interneurons (MLI). In some experiments sagittal slices were cut from the forebrain of 12 day old rats for recordings in cortical neurons with the same procedures. Slices were prepared in a solution containing (mM): 115 NaCl, 2.5 KCl,1.3 NaH_2PO_4, 26 $NaHCO_3$, 5 sodium pyruvate and 25 glucose. For slicing the solution contained 4 mM $MgCl_2$ and 0.5 mM $CaCl_2$ and for recovery 1 mM $MgCl_2$ and 2 mM $CaCl_2$. Both solutions were equilibrated with 95%O_2 - 5%CO_2.

2.2. Ethical approval

Sprague Dawley rats were provided by Janvier (St Berthevin, France) and subsequently housed at the central animal house at Université Paris Descartes (Centre St Pères, approval number A-750607), approved by the Prefecture de Police following inspection by Veterinary Services of the city of Paris, and representatives of the French Ministry of Research and the Ministry for Health, in agreement with the European Directive 86/609/EEC regarding the protection of animals used for experimental and other scientific purposes. Experimental procedures were approved by the Directorate of Paris Veterinary Services, by the scientific committee of the central

animal house of Paris Descartes (Centre St Pères) as well as by the ethical committee for animal experimentation of Université Paris Descartes.

2.3. Electrophysiological recording

A Hepes-buffered saline was used for recording, containing a low concentration of bicarbonate to maintain intracellular pH, composition (mM): 132 NaCl, 4 KCl, 2.5 $NaHCO_3$, 10 Hepes, 25 glucose and 5 sodium pyruvate, pH 7.3, usually with 1 mM $MgCl_2$ and 2 mM $CaCl_2$. For experiments with NMDA receptors Mg^{2+} ions were omitted and 50 mM glycine added. Hydrated oxygen was blown over the surface and also produced mixing of the cage in the bath solution. The intracellular solution for Purkinje neurons was (in mM): 135 potassium gluconate, 10 KCl, 10 Hepes, 0.1 EGTA, 4.6 $MgCl_2$, 4 $ATPNa_2$ and 0.4 GTPNa, pH adjusted to 7.3 with KOH and osmolality to 300 mosmol kg^{-1}. The intracellular solution for MLI was (mM): 150 KCl, 4.6 $MgCl_2$, 0.1 $CaCl_2$, 10 Hepes, 1 EGTA, 4 $ATPNa_2$ and 0.4 $GTPNa_2$, pH adjusted to 7.3 with KOH and osmolality to 300 mosmol kg^{-1}. Recordings were at room temperature.

The preparation was viewed with a Zeiss Axioskop1FS (Oberkochem, Germany) with Leica 40 x 0.8 w or 63 x 0.9 w objectives. To avoid photolysis, 500/40 nm bandpass illumination was used.

Recording pipettes had resistances of 2.5-4.5 MΩ for Purkinje neurons, 5-8MΩ for MLI. Whole cell voltage clamp recordings from Purkinje neurons were with a SEC-10LX switch clamp amplifier (NPI, Munich, Germany). Series resistance was 7-10 MΩ in Purkinje neurons and 13-18 MΩ in MLI. For recordings in MLI the amplifier was used in non-switching mode. The pipette potential was -60 mV, data were not corrected for the junction potential of 12 mV. Data acquisition was with a NI USB interface (National Instruments, Austin, Texas) sampled at 2 kHz or 10 kHz with WINWCP (Dr. John Dempster, University of Strathclyde) and analyzed in Igor Pro (Wavemetrics, Lake Oswego, Oregon).

For climbing fiber (CF) stimulation, cathodal pulses of 50 ms duration and supramaximal amplitude were delivered from a constant voltage stimulator through glass pipettes with 2.5-4.5MΩ resistance positioned at the surface of the slice in the granule cell layer. The stimulus comprised two pulses separated by 40 ms to test paired pulse depression. To reduce the inward current generated by the Purkinje neuron with CF stimulation the intracellular solution contained 5 mM QX314 and the extracellular solution 100 nM NBQX in these experiments.

2.4. Flash photolysis

Flash photolysis was through the transmitted light path with a xenon arc flashlamp (Rapp Optoelectronic, Hamburg, Germany) producing a 1 ms light pulse filtered 290-370 nm (UG11; Schott, Mainz, Germany) and focused by a silica condenser through the slice to illuminate a 200 µm diameter spot at the top surface. The lamp alignment and output were measured with a photodiode at the specimen plane before each experiment. During experiments the lamp was used at full output and the extent of photolysis varied with neutral density filters in the light path. Flashlamp photolysis was calibrated in the microscope with the caged fluorophore NPE-HPTS (50 µM; Tocris, UK) prepared as small aqueous vesicles (5-20 µm diam) suspended in Sylgard as described previously (Canepari et al., 2001a; Trigo et al., 2009a). The optical arrangement was as described by Canepari et al. (2001a) and the fraction of cage converted calculated as described there and by Trigo et al. (2009a). The conversions of NPE-ATP and MNI-glutamate relative to NPE-HPTS determined by Canepari et al. (2001a) were 5.0 and 3.1, respectively, and these values were used here. NPEC-caged ligands have the same photochemical properties of light absorption and quantum yield as NPE-ATP (Corrie et al., 1993) and the same conversion factor can be applied. None of the new cages used here contained additional chromophores that might affect the photochemical properties, hence the same conversion factors can be applied to each. The conversion of NPE-HPTS in the microscope described above was 14% with full lamp output

energy, corresponding to 70% conversion of the NPEC-caged ligands and 43% conversion of MNI-caged ligands, respectively. A further correction was required for transmission of photolysis light through the slice, estimated as 42% in the molecular layer of 20 day cerebellar slices at 200 µm thickness as used here (Canepari et al., 2004). The overall factors for conversion of NPEC-caged ligands and for MNI-caged ligands were 30% and 18%, respectively, at full flashlamp energy. To change the fractional conversion the intensity was reduced as appropriate by ND filters inserted in the light path.

Laser photolysis at 405 nm was used in some experiments with MNI-caged ligands with methods described previously (Trigo et al., 2009a). Here a large laser spot of 3 µm diameter was produced at the center of the CCD field by underfilling the back aperture of a 40 x 0.8 w objective (Leica, Germany). Low intensity pulses of duration 1-10 ms were used and intensity monitored with light reflected from the optical path onto a photodiode. The neuron was filled with 50 µM Alexa 594 (Invitrogen, France) added to the intracellular solution to permit identification by epifluorescence (excitation filter 572/35 nm, emission 640/70 nm Chroma, USA). The neuronal soma and dendrites were positioned relative to the laser spot by moving the recording table with 0.1 µm resolution by means of piezo drives. The light entering the objective was monitored with a photodiode and the calibration described by Trigo et al. (2009a) was applied to calculate the conversion of MNI-caged ligands at each intensity.

2.5. Drugs

Drugs used were CPCCOEt, D-AP5, SR 95531, TTX, NBQX, and QX314 from Tocris Bioscience UK. Agatoxin IVA and Cytochrome C were purchased from Sigma-Aldrich. GYKI 53655 was kindly provided by Dr. Michael Spedding.

3. Results

3.1. Tests for interference of the cage with synaptic transmission at climbing fiber to Purkinje neuron synapses

Each of the caged glutamate receptor ligands evaluated here was tested for interference with synaptic transmission when applied at concentrations that would be used in uncaging experiments. The climbing fiber-Purkinje neuron (CF,PN) connection in 18-20 day old rat cerebellum has a single input; this single input permitted tests for anesthetic effects of the caged ligands themselves on excitability by monitoring the threshold for nerve excitation, for interference with presynaptic release processes by testing paired pulse depression, and for interference with post-synaptic AMPA receptors by monitoring the post-synaptic response amplitude. If the caged ligand acts as an antagonist it is expected to decrease the amplitude of the evoked EPSC. Even low affinity antagonists such as ɣ-DGG or kynurenic acid have been shown to decrease the amplitude and slow the rise of PF-PN EPSCs at 1 mM concentration (Wadiche and Jahr, 2001).

To illustrate the experiments, Fig. 2 shows data obtained in the absence (black trace) or presence (gray trace) of 1 mM MNI-NMDA (Fig. 2A) or 100 µM MNI-kainate (Fig. 2B). Stimulation was with pairs of 50 ms pulses separated by 40 ms and delivered at 0.14 or 0.2 Hz. The threshold was determined in the absence and after 10 min in presence of 1 mM MNI-NMDA or 100 µM MNI-kainate. Thereafter stimuli were supramaximal. No change in the threshold for CF stimulation was found in the presence of either caged ligand (n = 3 experiments for each). Comparison of the records of Fig. 2 shows no change in the time-course or amplitude of CF responses in the presence of either caged ligand. The same protocol was applied for each of the caged ligands tested here and the data obtained are summarized in Table 1. The concentrations tested were those required in photolysis experiments to evoke large responses at full intensity of the flashlamp pulse. Each of the caged ligands tested here had no effect on the threshold for excitation of the CF or of the PN, or on the parameters tested of CF to PN synaptic transmission. A lack of interference with excitability and with synaptic transmission was reported previously for the caged L-glutamates

NPEC-L-glutamate (Corrie et al., 1993) and MNI-L-glutamate (Canepari et al., 2001a).

3.2. Varying the cage concentration at constant concentration of released ligand

A second test for interference with glutamate receptors by the caged ligands themselves was to maintain the ligand concentration released at a constant sub-maximal level by varying the light intensity reciprocally with the cage concentration as the latter was changed. Practically this was done by halving the cage concentration by dilution and doubling the intensity by changing neutral density filters in the light path.

The results of this protocol applied to photolysis of NPEC-DHPG are summarized in Fig. 3, which shows results from 5 cells. On average no change was seen in the amplitude of slow inward current evoked by 48 μM DHPG released in presence of 320 μM or subsequently 160 μM NPEC-DHPG. Similar tests were made with the caged ligands MNI-kainate, NPEC-AMPA and NPEC-ACPD. The results are summarized in Table 2. No evidence was found of strong interference by the cage on the response to the released ligand.

3.3. Caged ligands acting selectively at ionotropic glutamate receptors

Caged NMDA, caged kainate and caged AMPA were synthesized to permit selective activation of glutamate receptor sub-types without the need for presence of selective antagonists, as required when activated by L-glutamate released from MNI-caged glutamate. The caged NMDA and caged kainate tested here were the MNI-caged ligands; however the caged AMPA was the slower releasing NPEC cage because a synthesis of MNI-caged AMPA was not feasible, as the hydroxyisoxazole moiety in AMPA would not survive the nitration step that is integral to synthesis of MNI-caged amino acids (Papageorgiou and Corrie, 2002).

3.3.1. MNI-NMDA

MNI-NMDA photolysis was tested for stoichiometric photorelease of NMDA by quantitative amino acid analysis of the NMDA concentration following complete photolysis of a 1 mM solution of MNI-NMDA. 2 ml of 1 mM MNI-NMDA was photolyzed progressively in a photochemical reactor fitted with 350 nm lamps to 100% photolysis, monitored by UV-vis absorption spectroscopy as previously described (Papageorgiou and Corrie, 2000). The solution was split and one sample was subjected to amino acid analysis with ninhydrin detection (Department of Biochemistry, University of Cambridge). The other sample was subjected to bioassay by fast perfusion at NMDA receptors of hippocampal neurons. The release of NMDA assayed by amino acid analysis was 1.02 mM, while bioassay gave a similar value, 900 μM.

Photolysis of MNI-NMDA was also tested in molecular layer interneurons of the cerebellum, in external solution without Mg^{2+} ions and with 50 μM glycine present. The anatomical identification of MLI was confirmed by the characteristic large amplitude inward spontaneous synaptic currents seen with Cl^--containing internal solution and arising from GABA release. Responses to photoreleased NMDA were subsequently made at -60 mV with GABA receptors blocked by 10 μM SR 95531. Fig. 4A shows inward currents evoked by a low and a high concentration of NMDA photoreleased from 500 μM MNI-NMDA by a 1 ms pulse over a 200 μm field including the soma, dendrites and axon of the cell recorded. Both responses show the characteristic large increase of current noise seen with NMDA receptor activation. Fig. 4B shows the slow rise of the response to a high concentration of NMDA, with halftime10 ms, following release of NMDA uniformly over the field during the 1 ms flash. The blocking effect of adding 2 mM $MgCl_2$ extracellularly for a subsequent photolysis exposure after 5 min recovery is shown as the gray trace in Fig. 4B. Responses in MLI to photolysis of MNI-NMDA were similar when obtained in the presence or absence of 10 μM NBQX, showing that indirect activation by glutamate release did not contribute to the response. The current amplitude was small in these neurons and cell to cell variation of the current amplitude was large at each concentration of NMDA applied. Two responses were obtained

in each cell, consequently it was not possible to establish consistent concentration-response relations in single cells. Small responses were seen with low NMDA concentrations greater than 2.5 μM and maximal amplitude of inward current was seen with 90 μM released NMDA. A total of 12 MLI were tested. Localized laser photolysis to activate NMDA receptors was demonstrated in cortical neurons which generate large NMDA evoked currents. Fig. 4C shows responses to local NMDA photoreleased from 500 μM MNI-NMDA by 4 consecutive 10 ms pulses of 405 nm laser light at different intensities applied to the principal dendrite of a cortical pyramidal neuron. Under these conditions NMDA receptor activation was limited to a region of approximately 3 μm diameter. Laser intensity was increased in 4 equal steps of 0.1 mW to evoke sub-maximal and maximal activation of the NMDA receptor current. The responses are briefer than those seen with full field flashlamp photolysis because of rapid NMDA diffusion out of the small volume of the laser spot into the surrounding solution. The noise in the current records that results from the stochastic activation of large amplitude NMDA channel currents in the absence of external Mg^{2+} ions is seen in each trace.

3.3.2. MNI-kainate

Photolysis to release low concentrations of kainate from MNI-kainate with 1 ms flashlamp pulses delivered over the whole somatic and dendritic field of cerebellar Purkinje neurons evoked large inward currents of up to 2 nA amplitude at -60 mV potential. Kainate is known to activate both kainate and AMPA receptors (Wilding and Huettner, 1996). The sensitivity to kainate of cerebellar PN recorded in these experiments was high, as shown by the response to 1.4 μM kainate in Fig. 5A, suggesting the presence of substantial numbers of kainate receptors in PN. Because of the reported low selectivity of kainate in distinguishing kainate from AMPA receptors (reviewed by Traynellis et al., 2010) the AMPA receptor selective non-competitive inhibitor GYKI 53655 was used at 50 μM or 100 μM to determine the fraction of the current due to AMPA receptor activation by kainate as illustrated in Fig. 5A. At 50 μM GYKI 53655 the amplitude of the current was reduced to 64 ± 6% (SEM 5 cells) and at 100 μM to 60 ± 7% (SEM 8 cells) without changing the time-course of evoked current. Further addition of 30 μM NBQX completely suppressed the response to photoreleased kainate. The currents due to activation of kainate receptors by kainate concentrations in the range 0.2-3.6 μM in the presence of 50 μM GYKI 53655 are shown in the records of Fig. 5B. The full range of the concentration-response relation was not investigated because of poor voltage control in the Purkinje dendrites with inward currents larger than 1 nA. The peak inward current is plotted against kainate concentration in Fig. 5C. The results show that kainate release from MNI-kainate activates both kainate and AMPA receptors, about 40% of current in PN was due to AMPA receptors at low kainate concentrations. Thus, photoreleased kainate can be used at low concentration to selectively and efficiently activate kainate receptors in the presence of sub-type selective AMPA receptor antagonists such as GYKI 53655.

3.3.3. NPEC-AMPA

Synthesis of the fast-releasing cage MNI-AMPA was not feasible, consequently we synthesized NPEC-AMPA and characterized its photolysis. Although efficient, photolysis of NPEC-AMPA is expected to be rate-limiting at high concentration because of the slow photolysis rate following a light pulse (~ 10 s^{-1}, Corrie et al., 1993). Nevertheless, the time resolution will be better than is generally achieved with perfusion techniques, particularly in slice preparations.

AMPA was released at concentrations in the range 0.1- 6 μM by 1 ms flashlamp photolysis of 5-20 μM NPEC-AMPA present in the bath. Fig. 6A shows the inward current generated in a Purkinje neuron by flashlamp photolysis of 5 μM NPEC-AMPA to release 1.5 μM AMPA. This current was blocked by the presence of 30 μM NBQX. The selectivity for AMPA receptors was tested by photolysis in the presence of GYKI 53655 (50 or 100 μM). Photorelease of 1.5 or 3 μM AMPA, sufficient to generate inward currents larger than 1 nA in control, produced no response in

the presence of 50 μM GYKI. With a lower concentration of GYKI present, 15 μM, photorelease of AMPA generated transient inward currents of approximately 100 pA amplitude which were blocked by addition of 30 μM NBQX. The transient current at low GYKI concentration may be due to re-equilibration of GYKI at AMPA receptors upon photorelease of AMPA. The results show that selectivity of AMPA for AMPA receptors is high, and that photorelease of low concentrations of AMPA may be useful in selectively activating AMPA receptors when both AMPA- and kainate-preferring receptors are present. Furthermore, the AMPA-specific current did not show evidence of strong desensitization at the concentrations used here, although the possibility remains that a fast component in the 10 ms time range would have been missed because of the relatively slow photolysis rate.

3.4. Caged ligands acting at metabotropic glutamate receptors

The kinetics of signaling initiated by GPCR receptors are slow, on the timescale of 100 ms to seconds. Consequently, the slow photorelease of ligands from the NPEC caging group does not limit the rate of activation and therefore the time-course of downstream reactions can be inferred. Two ligands acting at mGluR receptors are described here, the non-selective mGluR agonist ACPD and the type 1 selective agonist DHPG. In Purkinje neurons these ligands are known to activate mGluR1 receptors generating a slow inward current similar to the slow EPSC mediated by mGluR1 receptors with parallel fiber stimulation (Batchelor et al., 1994; Canepari et al., 2001b).

3.4.1. NPEC-ACPD

Photorelease of ACPD from NPEC-ACPD evoked large inward currents at -60 mV rising to a peak on a 5 s timescale. Fig. 7A shows the response to 58 μM ACPD released with a 1 ms pulse in absence (black trace) and subsequently in the presence of 100 μM CPCCOEt, an inhibitor of type 1 mGluR receptors. The response was also inhibited reversibly by 1 mM MCPG. Fig. 7B shows the inward currents evoked by photorelease of ACPD at progressively higher concentrations, up to 30 μM, released from 100 μM NPEC-ACPD by pulses of increasing intensity at 5 min intervals. As the concentration of ACPD was increased in this range the rate of rise and peak amplitude increased. At high concentrations of ACPD the rate of decline was accelerated, an effect that may be due to activation of Ca^{2+}-dependent K conductances consequent upon Ca^{2+} entry in the cation channel mediating the slow inward current (Canepari et al., 2004).

3.4.2. NPEC-DHPG

Cerebellar Purkinje neurons have high densities of the metabotropic receptor mGluR1α which underlie the slow EPSP evoked by parallel fiber burst stimulation (Batchelor et al., 1994) and are important in motor coordination. DHPG is a selective agonist at mGluR1 and mGluR5 receptors. Fig. 8A shows the inward current evoked in a Purkinje neuron by photorelease of 48 μM DHPG from 320 μM NPEC-DHPG and the inhibition obtained in the presence of the type 1 mGluR1 antagonist CPCCOEt (gray trace). The dependence of the current amplitude on the DHPG concentration is illustrated by the records in Fig. 8B evoked consecutively at 5 min intervals to release 10 μM, 30 mM and 48 mM DHPG. The results from 4 cells of the inward current at -60 mV plotted against DHPG concentration are shown in Fig. 8C. To obtain consistent responses to photoreleased DHPG it was necessary to allow 5 min intervals between consecutive flashes and restrict the number of responses to 3 in each cell. This interaction between responses may have been due to persistence of released DHPG in the slice, which was not perfused.

3.5. Inhibition of GABA-mediated synaptic currents by caged glutamate receptor agonists

Although none of the caged ligands tested here was found to interfere with responses to CF stimulation, mediated mainly by the AMPA receptor sub-type of glutamate receptor, it is known that GABA-A receptors show greater susceptibility to interference by cages (Canepari et al., 2001a;

Molnár and Nadler, 2000; Trigo et al., 2009b; Fino et al., 2009). For this reason the block of GABA-mediated spontaneous miniature synaptic currents (mIPSC) by the caged ligands was tested here in molecular layer interneurons in cerebellar slices treated with TTX and NBQX in Mg^{2+}-containing solution. The amplitudes of miniature GABA-mediated inward currents at -70 mV were measured with KCl-based intracellular solution in the absence and presence of each of the cages at concentrations that would be used in photolysis experiments. The results obtained are summarized in Fig. 9. Fig. 9A shows the amplitude of mIPSCs as a ratio to the control obtained in the presence of MNI-L-glutamate concentrations up to 1 mM. To avoid the possibility of a bias arising from the threshold crossing used in event detection, the threshold was set conservatively at 50% maximum amplitude at each concentration, minimizing bias due to small events captured in control records but missed in the records with cage present when the amplitudes are reduced. The data for MNI-L-glutamate were fitted with a single binding inhibition curve giving an IC50 for MNI-L-glutamate inhibition of GABA-receptor synaptic current of 620 μM. At lower concentrations of 100 μM MNI-glutamate used in photostimulation experiments, the mean GABA-A receptor inhibition was 22%. Fig. 9B summarizes results with the MNI and NPEC cages determined in the same way in cerebellar interneurons or Purkinje cells. Data obtained at the maximum concentrations of the caged ligands used here are presented. MNI-kainate and MNI-NMDA showed levels of inhibition similar to those seen with MNI-glutamate. However, the MNIkainate concentrations used in photolysis experiments are lower because of the high potency of released kainate on kainate receptors. At 20 μM, the maximum concentration used in photolysis experiments described here, the inhibition of GABA-A receptors by MNI-kainate was 25%. MNI-NMDA had an IC50 of 500 μM. In contrast NPEC-DHPG, NPEC-ACPD and also NPEC-AMPA (not shown) produced no inhibition of GABA-A receptors at high concentrations.

4. Discussion

Several signaling pathways are initiated by ionotropic or metabotropic sub-types of receptors for the neurotransmitter L-glutamate. They differ in the glutamate concentrations required for activation, the kinetics and the downstream coupling to intracellular messengers, particularly to intracellular Ca^{2+} ion signaling. We describe here an evaluation of caged ligands acting selectively at sub-types of glutamate receptor that may be useful for pharmacological investigation of the receptor roles in signaling in the nervous system. Although the photorelease of L-glutamate itself in the presence of specific antagonists has provided experimental data on the properties and role of particular receptors and pathways (e.g. Canepari et al., 2001b), the presence of antagonists of receptor sub-types may conceal interactions between receptors or pathways that might be important in the physiological response to glutamate neurotransmission. For example the interactions demonstrated between NMDA and mGluR receptors (Perroy et al., 2008), and between AMPA receptors and mGluR receptors (Auger and Ogden, 2010) are modified by use of selective antagonists. The use of selective agonists allows pathways originating with different receptors to be activated and investigated independently.

Two photochemical caging strategies have been used here to generate hydrolytically stable caged amino acids. Where feasible, the fast-releasing nitroindoline photochemistry was used, based on the published syntheses (Papageorgiou et al., 1999; Papageorgiou and Corrie, 2002) applied here to NMDA and kainate to permit sub-ms ligand release. For metabotropic receptor ligands the fast rate is less important because of the slower timescale of GPCR signaling. In this case a caging group with simpler and more readily adapted synthesis was chosen, generating nitrophenylethoxycarbonyl derivatives of amino acids caged at the α-amino group as described for L-glutamate by Corrie et al. (1993). This strategy was applied to metabotropic receptor agonists ACPD and DHPG. The NPEC cages photolyze efficiently, with properties similar to caged ATP, NPE-ATP (Corrie et al., 1993; Walker et al., 1988) approximately 1.3 fold more efficiently than

MNIglutamate with flashlamp photolysis (Canepari et al., 2001a). However, the release rate following a pulse is 10-20 s^{-1}, corresponding to a half-time of 35-70 ms for ligand release.

The physiological rates of activation of AMPA receptors are high, however synthesis of the fast-releasing MNI-cage of AMPA proved intractable. The NPEC-AMPA tested here has slow release kinetics relative to AMPA receptor activation but nevertheless will be useful for the selective activation of AMPA receptors.

The chemical identities of the cages used here are supported by NMR, UV-vis spectroscopy and elemental analyses. Since there are no additional near-UV chromophores that might affect the photochemistry in the ligands caged here, the photochemical properties can be expected to be similar to those characterized for MNI-glutamate or NPEC-glutamate described previously (summarized in Trigo et al., 2009a; Corrie et al., 1993).

The intact caged ligands, i.e. without photolysis, were tested for unwanted actions on excitability, on glutamatergic synaptic transmission, on the target receptors themselves, and also on GABA receptors which are known to be sensitive to interference by caged amino acids. At concentrations used in photolysis experiments no interference was detected with excitability in the climbing fiber - Purkinje neuron transmission nor in the actions of the caged ligands at their specific receptors.

Inhibition of GABA-A receptors by nitroindoline cages has been reported (Canepari et al., 2001a; Trigo et al., 2009a,b; Fino et al., 2009) and was investigated here at interneuron synapses. MNI-glutamate was found to have an IC50 of 0.6 mM, similar to that reported by Fino et al. (2009) and also similar to the inhibition of GABA-A-receptors by DPNI-GABA (Trigo et al., 2009b). Similarly MNI-NMDA had an IC50 at about 500 μM. However, MNI-kainate has an IC50 estimated as 100 μM, but because of the high potency of kinate at kainate-preferring receptors much lower MNI-kainate concentrations are needed. Similar levels of GABA-A receptor inhibition have been reported with the ruthenium coordination cage Rubi L-glutamate (IC50 = 300 μM) (Fino et al., 2009). Rubi- GABA has been reported as useful only at concentrations <20 μM (Rial-Verde et al., 2008). In contrast, NPEC-caged ligands showed no inhibition at GABA-A receptors at concentrations used experimentally. For photostimulation or photoinhibition of individual neurons, MNI-L-glutamate and DPNI-GABA (Trigo et al., 2009b) can be used at low concentrations, 100 μM, with near-UV or 405 nm excitation with minimal interference at GABA-A receptors.

Neither MNI- nor NPEC-caging groups are excited efficiently by two-photon absorption (MNI-glutamate 0.06 GM; Matsuzaki et al., 2001; NPE-EGTA <0.01 GM; Brown et al., 1999). Two-photon cross-sections are small and would require high concentrations of cage with high intensity and prolonged illumination. Furthermore, for NPEC-caged ligands the slow uncaging reactions would delocalize release. Similarly, the Rubi caged L-glutamate has an estimated two-photon cross-section of 0.14, requiring high intensities and exposures in photostimulation experiments (Fino et al., 2009).

The selectivity of receptor activation depends on the agonist released and is independent of the caging group. Photoreleased NMDA acted only at NMDA receptors at the concentrations used here, permitting use in experiments to selectively activate NMDA receptors by photolysis when AMPA receptor mediated fast synaptic transmission is intact. In the case of AMPA released from NPEC-AMPA the released ligand was selective for AMPA receptors over kainate receptors in Purkinje neurons at concentrations up to 10 μM used here, sufficient to produce large inward currents in PN. However, the kainate released from MNI-kainate activated both kainate and AMPA receptors at low concentrations as expected from the reported EC50 values (Traynellis et al., 2010), requiring the presence of GYKI 53655 (or another AMPA receptor selective antagonist) to produce selective activation of kainate receptors. Photoreleased kainate at low concentration was able to generate substantial inward current in PN, suggesting a large number of post-synaptic kainate receptors.

The exogenous receptor-specific ligands released in the experiments described here are not transported and metabolized in the tissue, unlike the endogenous transmitters. They may therefore persist in the preparation to produce prolonged responses. We have previously determined that L-glutamate photoreleased by flashlamp photolysis over the full field in a slice recording has mean half-life of 212 ms adjacent to the recorded cell. This can be compared with loss from the same region of a non-endogenous fluorophore, HPTS photoreleased from caged HPTS, with half-time for diffusional loss of 40 s (D.O. and M. Canepari; unpublished data). This suggests that the removal of non-endogenous ligands by diffusion following flashlamp photolysis in a slice preparation will be slow. The persistence of the ligand will affect the time-course of receptor activation, prolonging the rise and the decline of the response. The activation of metabotropic receptors by photoreleased DHPG or ACPD seen here is slower than that seen with photoreleased glutamate (Canepari and Ogden, 2006). The interactions seen here between successive applications of ACPD or DHPG with flashlamp photolysis may be due to persistence of the ligands in the slice. In localized laser photorelease the quantities of released ligand are much less because of the small photolysis volume and are dispersed rapidly by diffusion out of the laser spot.

5. Conclusion

The ability to apply ligands selective for glutamate receptor subtypes with good time resolution, and with spatial localization by combining photolysis with laser microscopy, provides useful probes for receptor sub-type activation. The reagents described here are water soluble, efficient in near-UV photolysis, and have rates of release adapted to the target receptors. They have been tested at concentrations up to 1 mM and have pharmacological properties suitable for use as photolabile precursors of selective ligands for near-UV excitation.

Acknowledgments

Supported by the EU Strep “Photolysis” LSHM-CT-2007-037765 (All authors), the CNRS and ANR (FPC, C.A., D.O.), the GACR and AVOZ (309/07/0271 and 50110509; L.V, O.C) and UK Medical Research Council (J.E.T.C).

Appendix A. Supplementary information

Supplementary information associated with this article can be found, in the online version, at doi:10.1016/j.neuropharm.2012.05.010.

References

Auger, C., Ogden, D., 2010. AMPA receptor activation controls type I metabotropic glutamate receptor signalling via a tyrosine kinase at parallel fibre-Purkinje cell synapses. J. Physiol. 588, 3063-3074.

Batchelor, A.M., Madge, D.J., Garthwaite, J., 1994. Synaptic activation of metabotropic glutamate receptors in the parallel fibre-Purkinje cell pathway in rat cerebellar slices. Neuroscience 63, 911-915.

Brown, E.B., Shear, J.B., Adams, S.R., Tsien, R.Y., Webb, W.W., 1999. Photolysis of caged calcium in femtoliter volumes using two-photon excitation. Biophys. J. 76, 489-499.

Canepari, M., Nelson, L., Papageorgiou, G., Corrie, J.E.T., Ogden, D., 2001a. Photochemical and pharmacological evaluation of 7-nitroindolinyl and 4-methoxy-7-nitroindolinyl amino acids as novel, fast caged neurotransmitters. J. Neurosci. Methods 112, 29-42.

Canepari, M., Papageorgiou, G., Corrie, J.E.T., Watkins, C., Ogden, D., 2001b. The conductance underlying the parallel fibre slow EPSP in rat cerebellar Purkinje neurones studied with photolytic release of L-glutamate. J. Physiol. 533.3, 765-772.

Canepari, M., Auger, C., Ogden, D., 2004. Ca^{2+} ion permeability and single-channel properties of the metabotropic slow EPSC of rat Purkinje neurons. J. Neurosci. 24, 3563-3573.

Canepari, M., Ogden, D., 2006. Kinetic, pharmacological and activity-dependent separation of two Ca^{2+} signalling pathways mediated by type 1 metabotropic glutamate receptors in rat Purkinje neurones. J. Physiol. 573, 65-82.

Corrie, J.E.T., DeSantis, A., Katayama, Y., Khodakhah, K., Messenger, J., Ogden, D., Trentham, D.R., 1993. Postsynaptic activation at the squid giant synapse by photolytic release of L-glutamate from a 'caged' L-glutamate. J. Physiol. 465, 1-8.

DiGregorio, D.A., Rothman, J.S., Nielsen, T.A., Silver, R.A., 2007. Desensitization properties of AMPA receptors at the cerebellar mossy fiber granule cell synapse. J. Neurosci. 27, 8344-8357.

Fino, E., Araya, R., Peterka, D.S., Salierno, M., Etchenique, R., Yuste, R., 2009. RuBi-glutamate: two-photon and visible-light photoactivation of neurons and dendritic spines. Front. Neural Circuits 3, 2.

Gasparini, S., Magee, J.C., 2006. State-dependent dendritic computation in hippocampal CA1 pyramidal neurons. J. Neurosci. 26, 2088-2100.

Heinbockel, T., Brager, D.H., Reich, C.G., Zhao, J., Muralidharan, S., Alger, B.E., Kao, J.P.Y., 2005. Endocannabinoid signaling dynamics probed with optical tools. J. Neurosci. 25, 9449-9459.

Jabs, R., Matthias, K., Grote, A., Grauer, M., Seifert, G., Steinhäuser, C., 2007. Lack of P2X receptor mediated currents in astrocytes and GluR type glial cells of the hippocampal CA1 region. Glia 55, 1648-1655.

Khodakhah, K., Ogden, D., 1995. Fast activation and inactivation of inositol trisphosphate-evoked Ca^{2+} release in rat cerebellar Purkinje neurones. J. Physiol. 487, 343-358.

Matsuzaki, M., Ellis-Davies, G.C.R., Nemoto, T., Miyashita, Y., Iino, M., Kasai, H., 2001. Dendritic spine geometry is critical for AMPA receptor expression in hippocampal CA1 pyramidal neurons. Nat. Neurosci. 4, 1086-1092.

Molnár, P., Nadler, J.V., 2000. Gamma-Aminobutyrate, alpha-carboxy-2-nitrobenzyl ester selectively blocks inhibitory synaptic transmission in rat dentate gyrus. Eur. J. Pharmacol. 391, 255-262.

Morrison, J., Wan, P., Corrie, J.E.T., Papageorgiou, G., 2002. Mechanisms of photorelease of carboxylic acids from 1-acyl-7-nitroindolines in solutions of varing water content. Photochem. Photobiol. Sci. 1, 960-969.

Murphy, K.P.S.J., Williams, J.H., Bettache, N., Bliss, T.V.P., 1994. Photolytic release of nitric oxide modulates NMDA receptor-mediated transmission but does not induce long-term potentiation at hippocampal synapses. Neuropharmacology 33, 1375-1385.

Papageorgiou, G., Corrie, J.E.T., 2000. Effects of aromatic substituents on the photocleavage of 1-acyl-7-nitroindolines. Tetrahedron 56, 8197-8205.

Papageorgiou, G., Corrie, J.E.T., 2002. Regioselective nitration of 1-acyl-4-methoxyindolines leads to efficient synthesis of a photolabile L-glutamate precursor. Synth. Commun. 3, 1571-1577.

Papageorgiou, G., Ogden, D., Barth, A., Corrie, J.E.T., 1999. Photorelease of carboxylic acids from 1-acyl-7-nitroindolines in aqueous solution: rapid and efficient photorelease of L-glutamate. J. Am. Chem. Soc. 121, 6503-6504.

Perroy, J., Raynaud, F., Homburger, V., Rousset, M.C., Telley, L., Bockaert, J., Fagni, L., 2008. Direct interaction enables cross-talk between ionotropic and group I metabotropic glutamate receptors. J. Biol. Chem. 283, 6799-6805.

Rial-Verde, E., Zayat, L., Etchenique, R., Yuste, R., 2008. Photorelease of GABA with visible light using an inorganic caging group. Front. Neural Circuits 3, 2-8.

Traynellis, S.F., Wollmuth, L.P., McBain, C.J., Menitti, F.S., Vance, K.M., Ogden, K.K., Hansen, K.B., Yuan, H., Myers, S.J., Dingledine, R., 2010. Glutamate receptor ion channels: structure, regulation and function. Pharmacol. Rev. 62, 405-496.

Trigo, F.F., Corrie, J.E.T., Ogden, D., 2009a. Laser photolysis of caged compounds at 405 nm: photochemical advantages, localisation, phototoxicity and methods for calibration. J. Neurosci. Methods 180, 9-21.

Trigo, F.F., Papageorgiou, G., Corrie, J.E.T., Ogden, D., 2009b. Laser photolysis of DPNI-GABA, a tool for investigating the properties and distribution of GABA receptors and for silencing neurons in situ. J. Neurosci. Methods 181, 159-169.

Wadiche, J.I., Jahr, C.E., 2001. Multivesicular release at climbing fiber-Purkinje cell synapses. Neuron 32, 301-313.

Walker, J.W., Reid, G.P., McCray, J.A., Trentham, D.R., 1988. Photolabile 1-(2-nitrophenyl)ethyl phosphate esters of adenine nucleotide analogues. Synthesis and mechanism of photolysis. J. Am. Chem. Soc. 110, 7170-7177.

Wilding, T.J., Huettner, J.E., 1996. Antagonist pharmacology of kainate- and alpha-amino-3-hydroxy-5-methyl-4-isoxazolepropionic acid-preferring receptors. Mol. Pharmacol. 49, 540-546.

Fig. 1. Reactions and structures of the reagents tested here. Panel A: Structures of MNI- and NPEC-caged compounds. MNI-glutamate is also shown for reference. Panel B: Photolysis reactions for NPEC-glutamate (Corrie et al., 1993) and MNI-L-glutamate (Morrison et al., 2002) respectively.

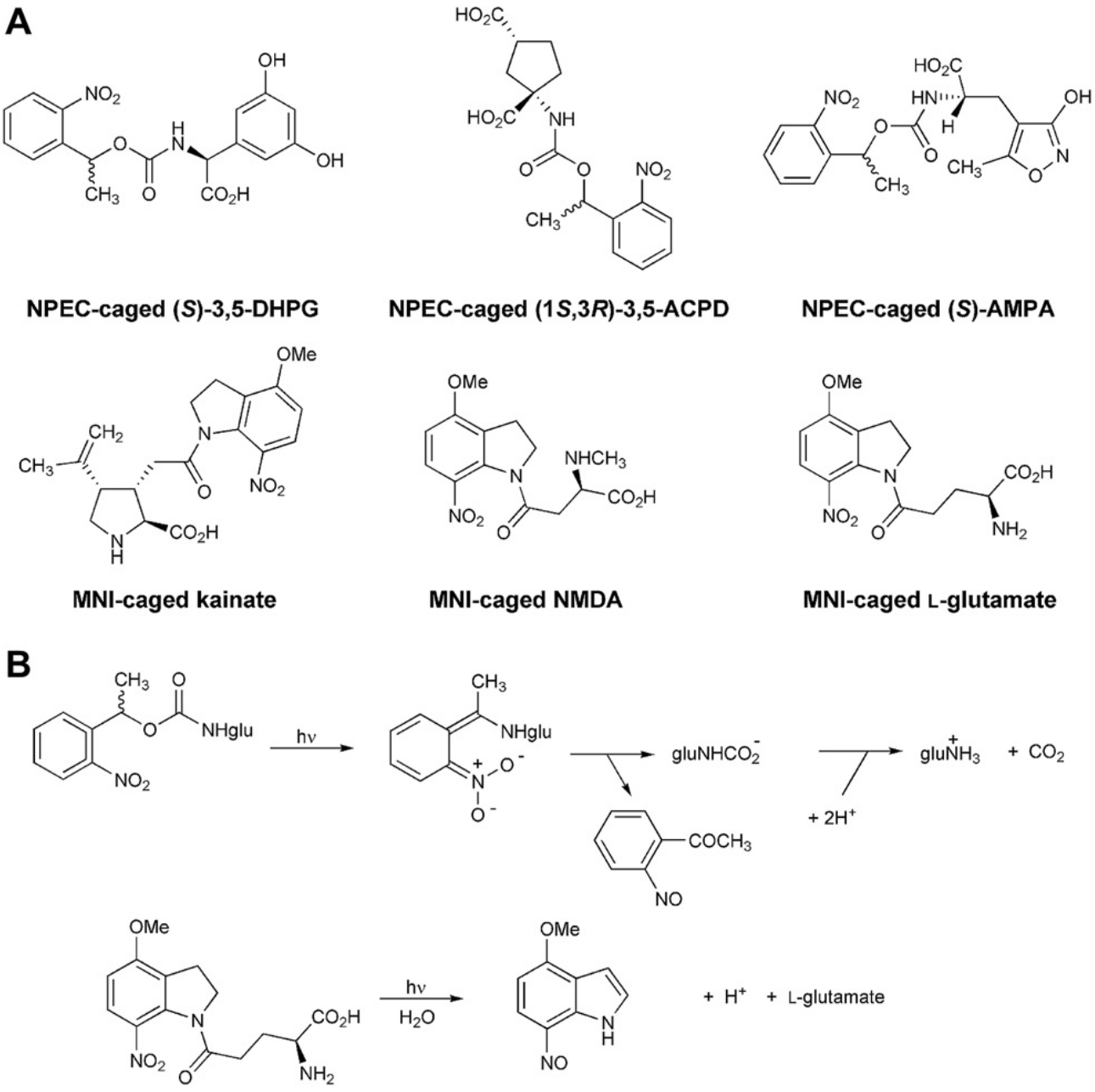

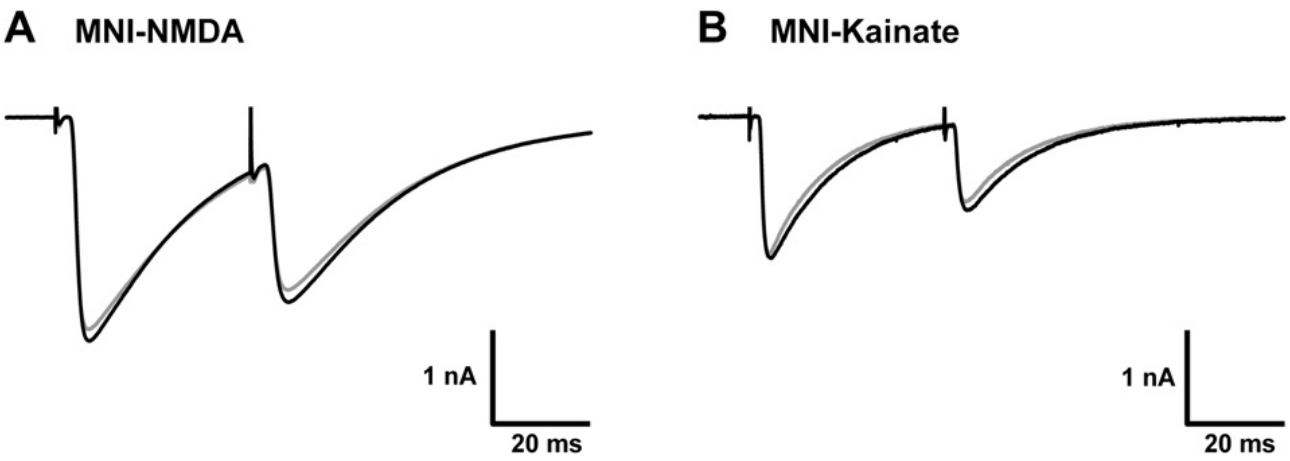

Fig. 2. Tests for an effect of MNI-caged NMDA or MNI-caged kainate on climbing fiber transmission to Purkinje neurons. Each panel shows averages of 10 sweeps obtained in the absence (black traces) or presence (gray traces) of 1 mM MNI-NMDA (Panel A) or 100 μM MNI-kainate (Panel B). Recording from 18 to 20 day old Purkinje neurons. 100 nM NBQX was present to reduce the amplitude of CF evoked inward current to 1-2 nA.

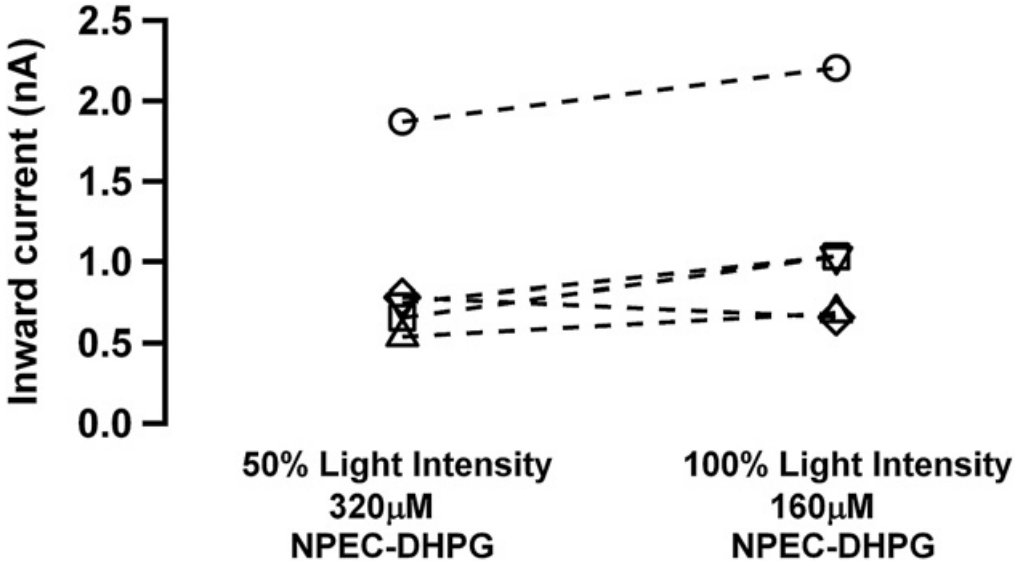

Fig. 3. Tests for interference of the cage with glutamate receptors: effect of halving the cage concentration while doubling the flash intensity. Results of 5 experiments in which NPEC-DHPG at 320 μM was photolyzed with 50% light intensity to release 48 μM DHPG and subsequently diluted 2 fold to release 48 μM at 100% intensity in the presence of 160 μM NPEC-DHPG. Mean peak inward currents recorded at -60 mV pipette potential.

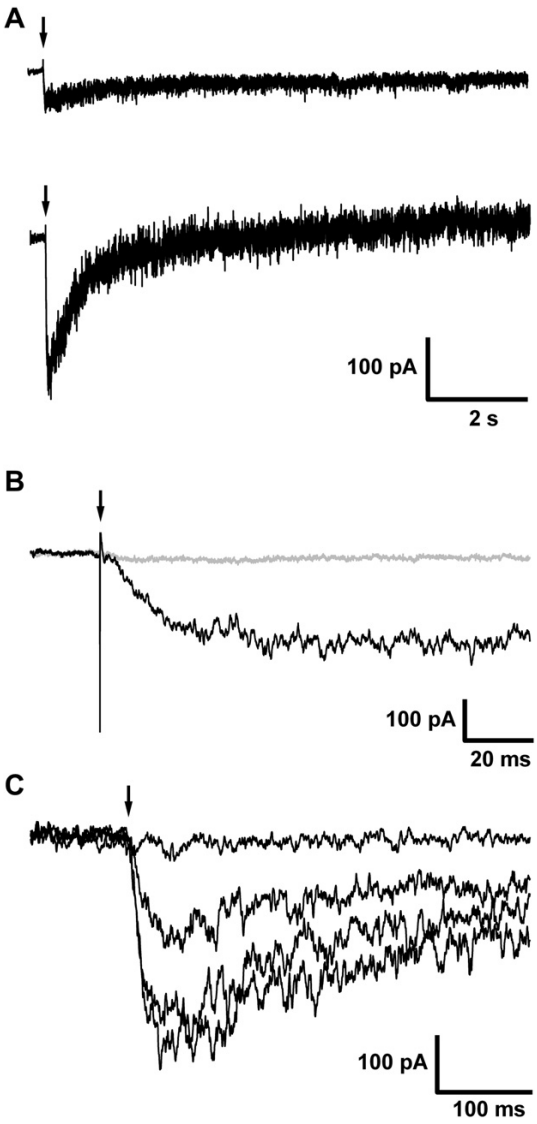

Fig. 4. Responses to photorelease of NMDA from MNI-NMDA. Panel A shows the inward current evoked in a cerebellar molecular layer interneuron following photolysis with a 1 ms flashlamp pulse to release NMDA at low (23 μM, upper record) or high concentration (45 μM, lower record) at the time indicated by the arrows. Pipette potential -60 mV, Mg^{2+}-free external solution. Panel B shows the response to a high concentration 45 μM NMDA (black trace) on an expanded timescale following a 1 ms flashlamp pulse. The gray trace shows the record obtained after adding 2 mM Mg^{2+} to the external solution. Panel C shows responses in a cortical pyramidal neuron to photolysis in a 3 μm diameter laser spot at 405 nm applied consecutively at 4 different intensities for 10 ms (time indicated by the arrow) to the origin of the main dendrite. Potential 60 -mV, Mg^{2+}-free saline, 500 μM MNI-NMDA present in the external solution, NMDA concentrations released approx. 10, 20, 50 and 100 μM. Data are lowpass filtered at 500 Hz.

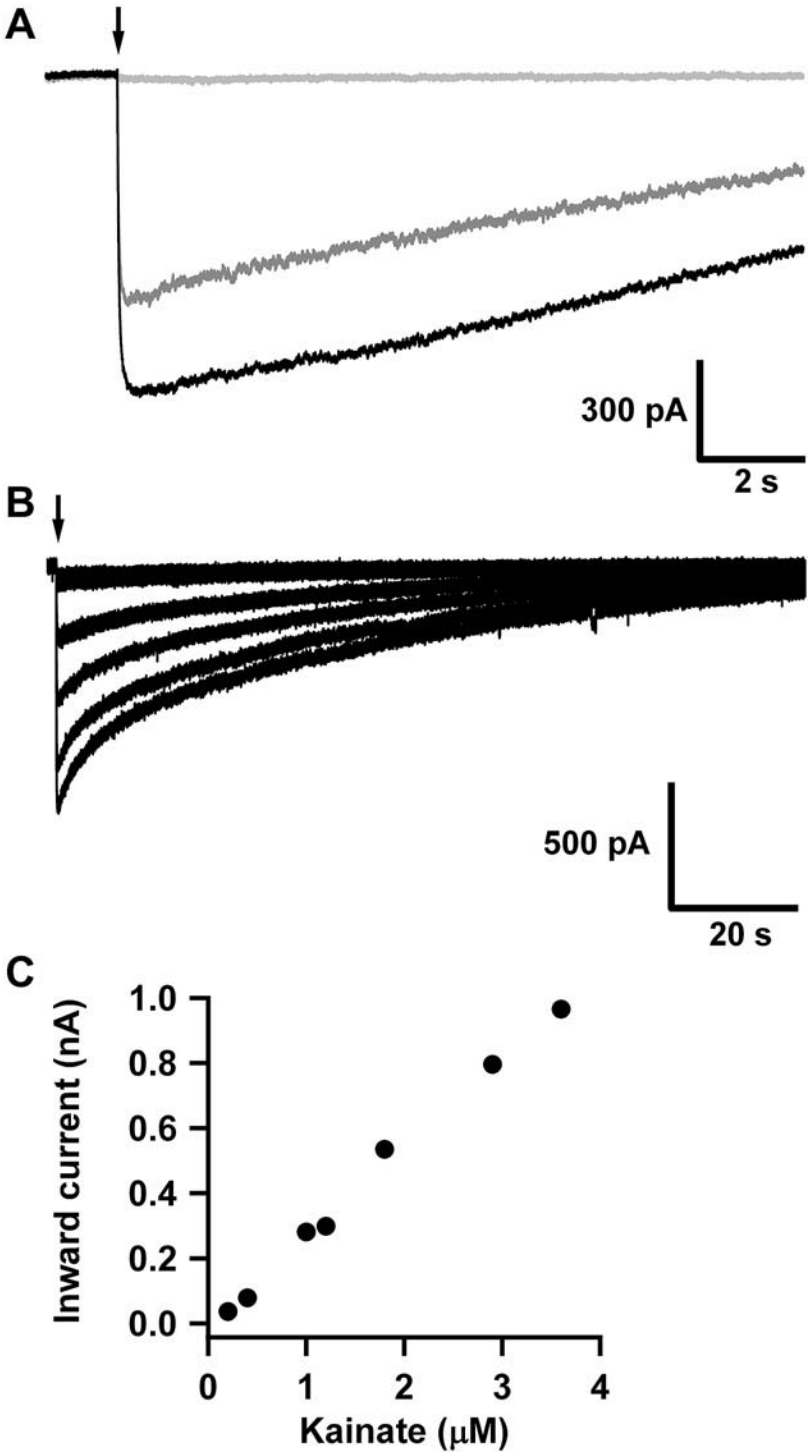

Fig. 5. Responses of cerebellar Purkinje neurons to photorelease of kainate from MNI-kainate. Panel A shows the current recorded at -60 mV in response to release of 1.4 μM kainate from 10 μM MNI-kainate in absence (black trace) or presence of AMPA receptor blocker GYKI 53655 (50 μM; dark gray trace) and with the additional presence of 30 μM NBQX (sufficient to block all AMPA-kainate receptors; light gray trace). Panel B shows the currents recorded at progressively greater flashlamp intensities, releasing progressively higher kainate concentrations up to 3.6 μM from 20 μM MNIkainate. In Panel C the peak inward currents are plotted against released kainate concentration. Experiments in B and C were in presence of 50 μM GYKI 53655.

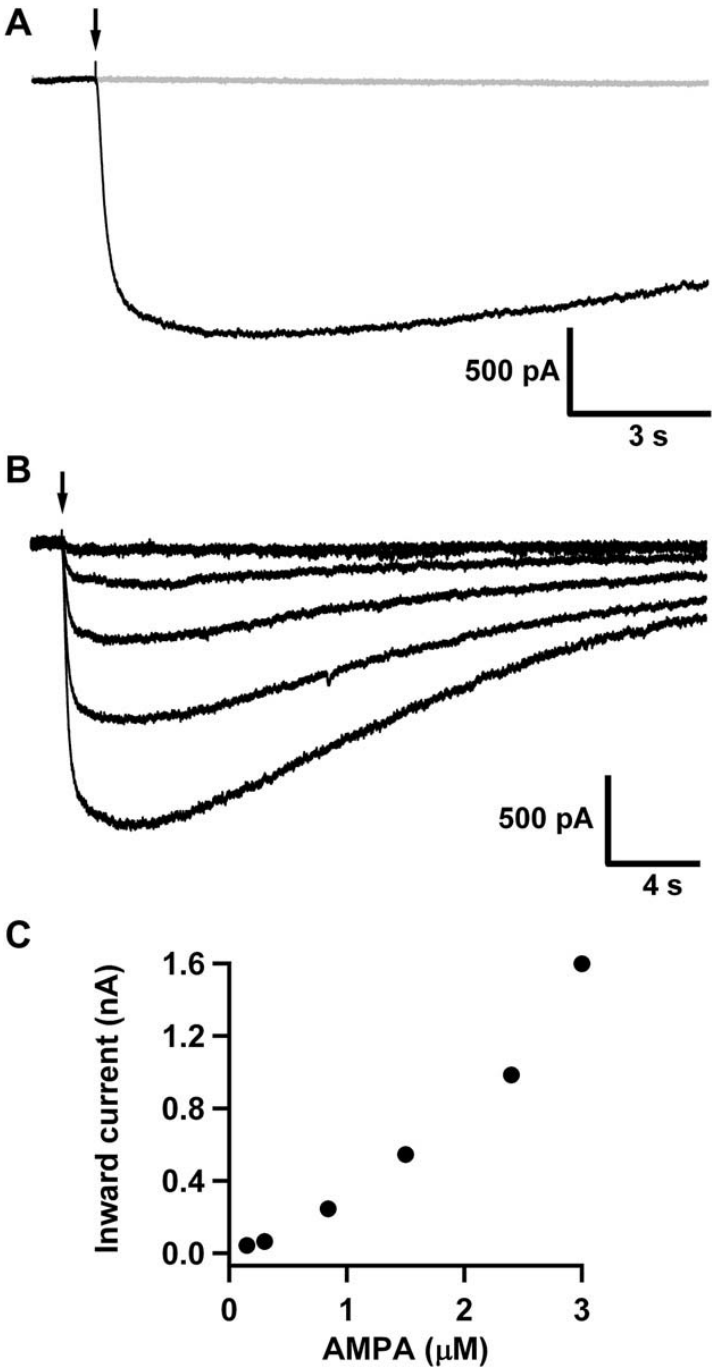

Fig. 6. Inward current recorded in a Purkinje neuron following photorelease of AMPA from NPEC-caged AMPA. Holding potential -60 mV, 1 ms flashlamp pulses at the time indicated by the arrow. Panel A: 5 μM NPEC-AMPA photolyzed to release 1.5 μM AMPA in the absence (black trace) or presence (gray trace) of 30 μM NBQX. Panel B: Inward currents evoked by progressive increase of intensity of the photolysis pulse with 10 μM NPEC-AMPA present. Panel C: Peak inward current plotted against the AMPA concentration released by photolysis.

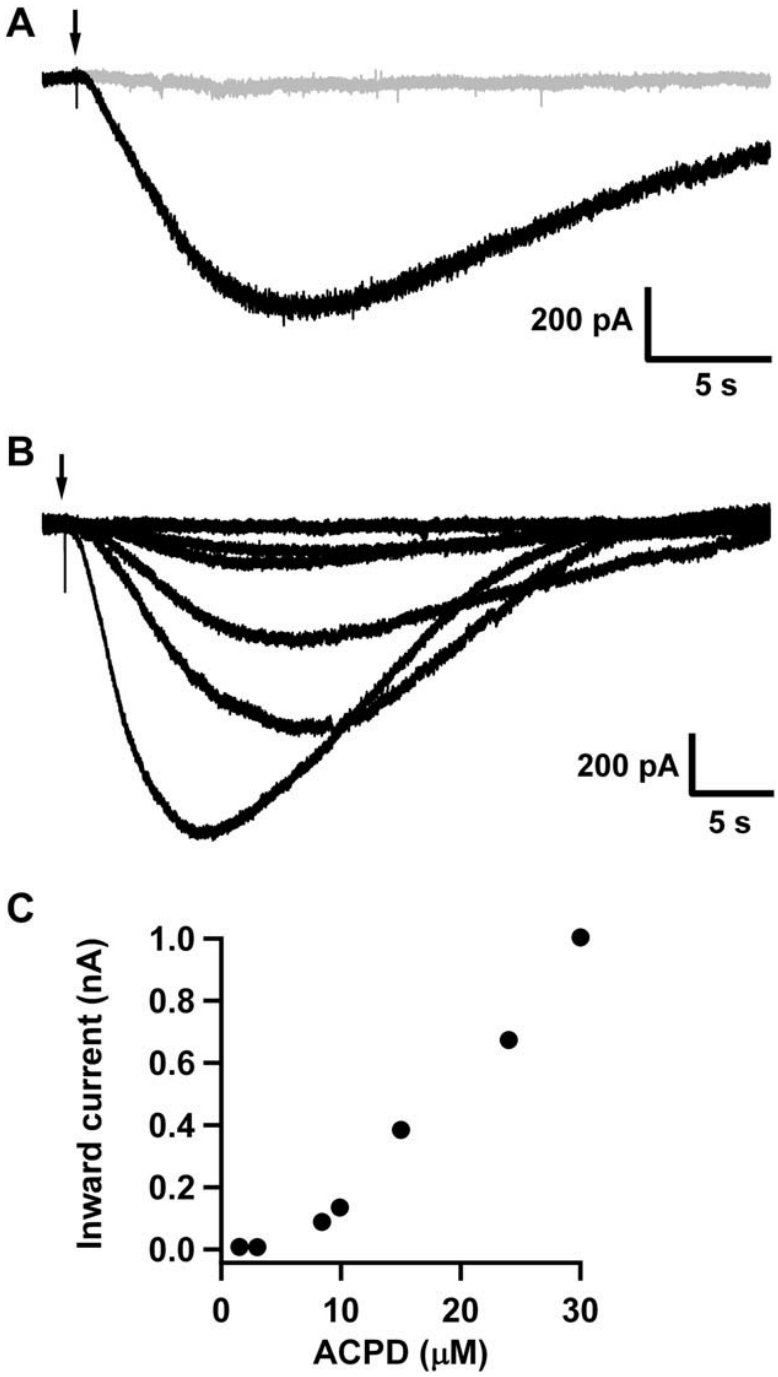

Fig. 7. Current evoked by photolysis of NPEC-ACPD in Purkinje neurons at -60 mV. Panel A shows the response to a high concentration of ACPD (58 μM) released from 240 μM NPEC-ACPD in absence (black trace) or presence of 100 μM CPCCOEt (gray trace). Panel B shows inward currents evoked by 1 ms flashlamp pulses of progressively increasing intensity elicited at 5 min intervals. Panel C shows the peak current plotted against the ACPD concentration in the range 1.5 μM-30 μM).

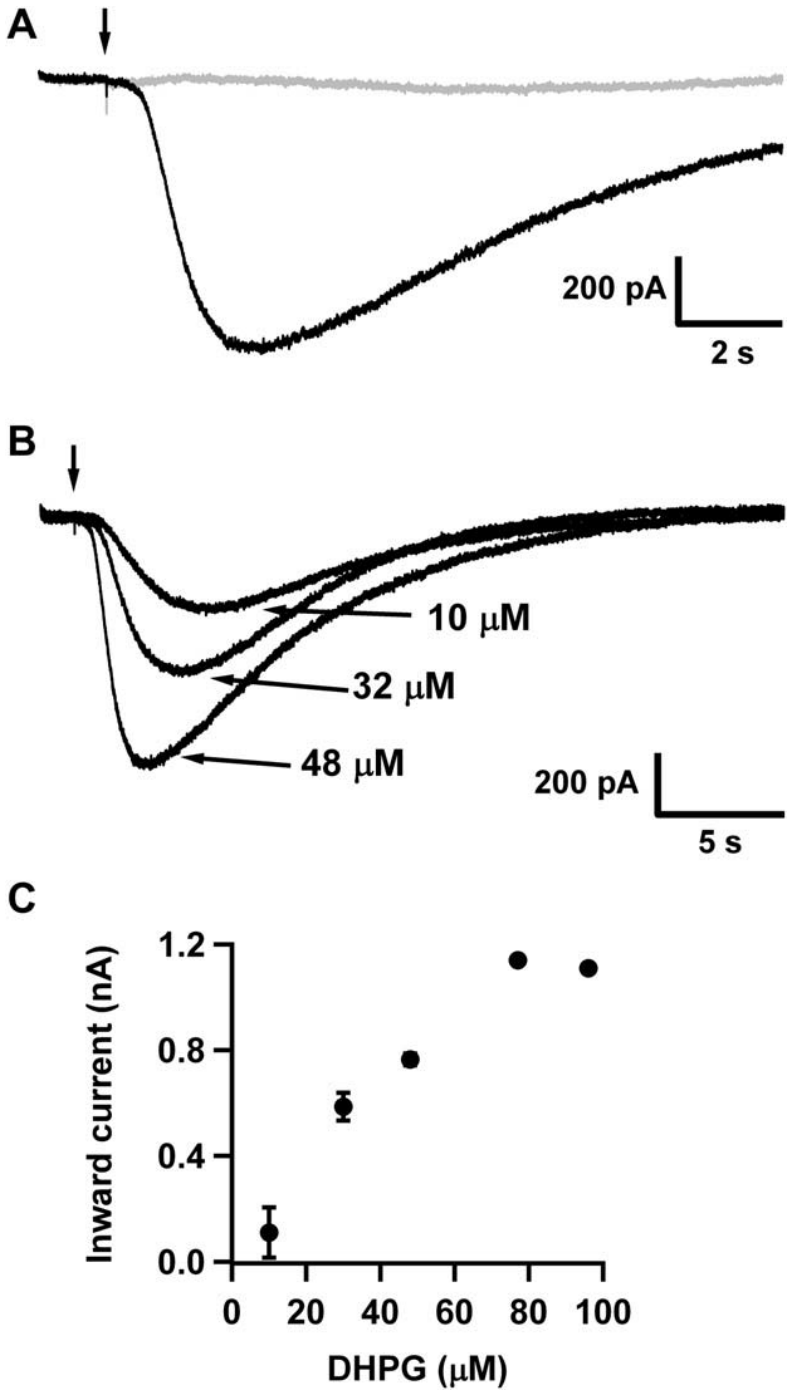

Fig. 8. Activation of mGluR receptors by photorelease of DHPG from NPEC-DHPG. Cerebellar Purkinje neurons, -60 mV. Panel A, inward current evoked by 48 μM DHPG photoreleased from 320 μM NPEC-DHPG in absence (black trace) or presence (gray trace) of 100 μM CPCCOEt. Panel B, inward current evoked by release of 10 μM, 32 μM or 48 μM DHPG consecutively in the same cell at 5 min intervals. Panel C, inward current evoked by photorelease of DHPG plotted against DHPG concentration (10 μM-96 μM). Mean SEM from 4 cells.

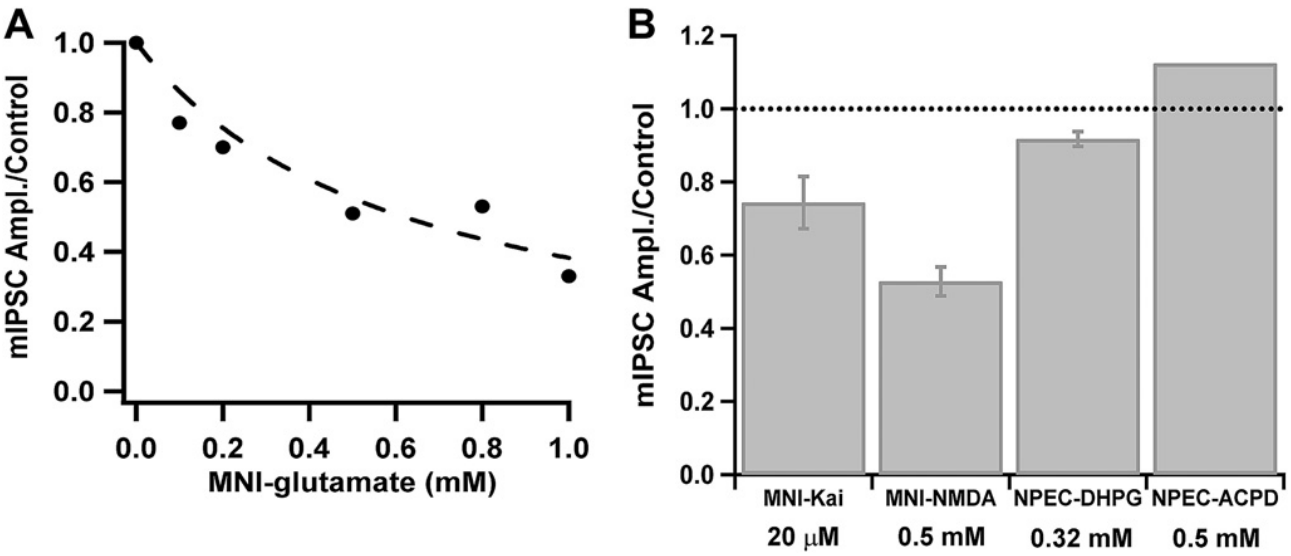

Fig. 9. Inhibition of GABA-A receptors by caged ligands. A. Inhibition by MNI-glutamate of GABA-A mediated currents in MLI. mIPSCs were recorded in presence of 2 μM TTX and 10 μM NBQX at -70 mV. Data in each experiment were normalized to control. Points are the mean of 3 observations at each concentration from 4 cells (>200 events in each). The mIPSCs were detected with a threshold set at 50% maximum amplitude to avoid sampling bias due to greater inhibition at high cage concentrations. An IC50 of 0.62 mM was determined for the inhibition curve y = IC50/(x + IC50) fitted with weighted least-squares to the data (y is the fractional inhibition and x the concentration of cage). B. Inhibition of GABA mIPSCs at the maximum cage concentrations used in experiments (indicated beneath columns). Protocols as for Fig. 9A. Data from cerebellar interneurons and Purkinje neurons are combined.

Table 1 Effect of caged neuroactive amino acids on transmission at the climbing fiber-Purkinje neuron synapse.

Caged-ligand	No. of cells	Control			Caged ligand present - ratios to control		
		Threshold V	Amplitude nA	PPR	Threshold	Amplitude	PPR
MNI-kainate 100 μM	3	9±4.3	1.8±0.28	0.6±0.03	No change	0.93±0.04	1.0±0.03
MNI-NMDA 1 mM	3	14±1.7	1.9±0.97	0.8±0.06	No change	0.95± 0.04	0.99±0.01
NPEC-AMPA 200 μM	4	7±1.9	0.5±0.28	0.7±0.08	No change	0.94±0.05	1.0±0.03
NPEC-DHPG 320 μM	4	4±0.05	2.2±1.5	0.7±0.11	No change	0.93±0.12	0.97±0.08
NPEC-ACPD 1 mM	3	12±7.8	1.7±0.18	0.7±0.07	No change	0.99±0.07	0.99±0.01

The threshold for CF stimulation, the amplitude of EPSC for the first pulse and the paired pulse ratio (PPR) at 40 ms interval are shown for each cage at the concentration indicated. In presence of the cage (right hand columns) data are reported as the fractional change (SD) seen in each cell in presence of the cage at the concentration indicated. The experiments were performed in the presence of 100 nM NBQX.

Table 2 Summary of the effect of reducing the cage concentration at constant ligand concentration for 4 caged ligands.

Initial concentrations of cage and the concentration of released ligand	No of cells	50% intensity at 100% cage concentration		Fraction of control 100% intensity at 50% cage concentration	
		Mean amplitude	SEM	Mean fraction	SEM
NPEC-DHPG 320 μM (DPHG 48 mM)	5	-0.92 nA	0.24	1.2	0.21
NPEC-ACPD 200 or 100 μM (ACPD 30 or 15 mM)	5	-1.15 nA	0.13	0.95	0.15
NPEC-AMPA 5 μM (AMPA 0.75 μM)	4	-0.60 nA	0.19	1.09	0.32
MNI-Kainate 20 μM (Kainate 1.8 μM)	2	-0.63 nA	-	0.98	-

Left column gives the initial cage concentration and the concentration of ligand released by the flash (in parenthesis). Mean amplitude is the peak current at -60 mV in 2-5 cells. The right panels are the fractional change in the peak current in each cell after diluting the cage 2 fold and doubling the flash intensity. Experimental protocol as described for Fig. 2 legend.

Supplementary Information

NPEC-caged Ligands. The NPEC-caged ligands described here were prepared using methods based on the published synthesis of NPEC-caged glutamate (Corrie et al., 1993). In all cases the compounds were obtained as diastereoisomeric mixtures because the 1-(2-nitrophenyl)ethanol used as a starting material was racemic. The diastereoisomerism arises only from the presence of two stereoisomers in the caged portion of the molecule, and the conditions of synthesis do not affect the chirality of the neurotransmitter component. Thus the photoreleased neurotransmitter analogue is stereochemically pure in all cases.

NPEC-caged ACPD
(1*S*,3*R*)-1-({[1-(2-nitrophenyl)ethoxy]carbonyl}amino)cyclopentane-1,3-dicarboxylic acid

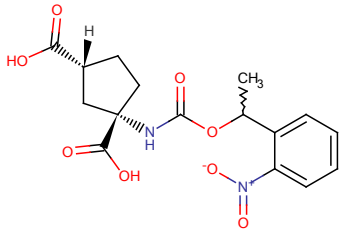

Prepared in four synthetic steps from (1*S*, 3*R*)-ACPD ex Tocris stock.
^{1}H NMR (300 MHz) d_6-DMSO, δ 12.25 (broad, ex, 2H), 8.00 (d, 1H), 7.85 (m, 2H), 7.70 (m, 1H), 7.55 (m, 1H), 5.95 (m, 1H), 2.80 (m, 1H), 2.40 (m, 1H), 2.05 (m, 1H), 1.85 (m, 4H), 1.50 (d, 3H).
MS: ES$^+$ m/z 389.21 [M+Na], 100%.
Anal. Calcd for $C_{16}H_{18}N_2O_8.0.25H_2O$: C, 51.82; H, 5.03; N, 7.55. Found: C, 51.70; H, 5.09; N, 7.67.
HPLC: >99%. Luna C18 3 µ 100 × 4.6 mm i.d. column. Column temp. = 25°C, flow rate = 1 mL/min, detection wavelength 261 nm.
Gradient: 10-100% MeCN + TFA (0.1% v/v): TFA (0.1% v/v aq.) in 20 min. Held at 100% MeCN + TFA (0.1% v/v) for 10 min. t_R 8.54 min.
Isocratic: 24% MeCN + TFA (0.1% v/v) : 76% TFA (0.1% v/v aq.) for 30 min. t_R 11.13 min.

NPEC- DHPG
(2*S*)-2-(3,5-dihydroxyphenyl)-2-({[1-(2-nitrophenyl)ethoxy]carbonyl}amino)acetic acid

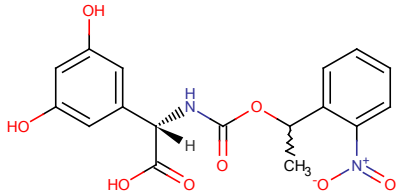

Prepared in four synthetic steps from (2*S*)-3,5-DHPG ex Tocris stock.
^{1}H NMR (300 MHz) d_6-DMSO, δ 12.75 (broad, ex, 1H), 9.30 (s, ex, 1H), 9.25 (s, ex, 1H), 8.00 (m, 2H), 7.80 (m, 1H), 7.75 (d, ex, 1H), 7.55 (m, 1H), 6.20 (dd, 2H), 6.15 (dd, 1H), 6.00 (m, 1H), 5.75 (m, 1H), 1.55 and 1.50 (2xd*, total 3H).
* Due to diastereomers.
MS: ES$^+$ m/z 398.90 [M+Na], 28%. ES$^-$ m/z 374.89 [M-H], 62%.
Anal. Calcd for $C_{17}H_{16}N_2O_8.0.50H_2O$: C, 52.99; H, 4.45; N, 7.27. Found: C, 52.85; H, 4.47; N, 7.05.
HPLC: >98%. Ascentis Express C18 2.7 µ; 100 × 4.6 mm i.d. column. Column temp. = 25 °C, flow rate = 1 mL/min, detection wavelength 270 nm.
Gradient: 10-100% MeCN + TFA (0.1% v/v): TFA (0.1% v/v aq.) in 10 min. Held at 100% MeCN + TFA (0.1% v/v) for 5 min. t_R 4.20 min.
Isocratic: 27.5% MeCN + TFA (0.1% v/v) : 72.5% TFA (0.1% v/v aq.) for 15 min. t_R 3.48 min.

NPEC--AMPA

(2*S*)-3-(3-hydroxy-5-methyl-1,2-oxazol-4-yl)-2-({[1-(2-nitrophenyl)ethoxy]carbonyl}amino)propanoic acid

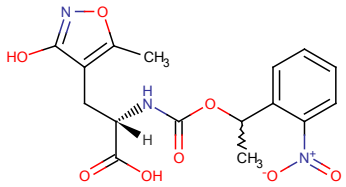

Prepared in four synthetic steps from (*S*)-AMPA ex Tocris stock.
^{1}H NMR (300 MHz) $CDCl_3$, δ 9.95 (v. broad, ex, 2H), 7.85 (d, 1H), 7.50 (m, 2H), 7.35 (m, 1H), 6.20 (m, 1H), 5.75 (m, 1H), 4.40 (m, 1H), 2.85 (m, 2H), 1.95 (s, 3H), 1.55 (d, 3H).
MS: ES+ m/z 401.90 [M+Na], 100%.
Anal. Calcd for $C_{16}H_{17}N_3O_8.0.5H_2O$ (also contained 0.18 entrained EtOAc): C, 49.69; H, 4.85; N, 10.40. Found: C, 49.80; H, 4.60; N, 10.22.
HPLC: Sum of two diastereomers = >99%. Luna C18 3 µ 100 × 4.6 mm i.d. column. Column temp. = 35 °C, flow rate = 1 mL/min, detection wavelengths 210 nm and 258 nm.
Gradient: 10-100% MeCN + TFA (0.1% v/v): TFA (0.1% v/v aq.) in 20 min. Held at 100% MeCN + TFA (0.1% v/v) for 10 min. Compound elutes as two diastereomers, t_R 9.09 and 9.17 min.
Isocratic: 27.5% MeCN + TFA (0.1% v/v) : 72.5% TFA (0.1% v/v aq.) for 30 min. Compound elutes as two diastereomers, t_R 9.51 and 9.98 min.

MNI-caged Ligands. The MNI-caged ligands described here were prepared using methods based on the published synthesis of MNI-caged glutamate and related compounds (Papageorgiou and Corrie, 2000, 2002; Papageorgiou, Ogden and Corrie, 2004). Unlike the NPEC-caged species, the cage group does not contain an asymmetric centre so the caged ligands are obtained as single optical isomers.

MNI-caged Kainate

(2*S*,3*S*,4*S*)-3-[2-(4-methoxy-7-nitro-2,3-dihydro-1*H*-indol-1-yl)-2-oxoethyl]-4-(prop-1-en-2-yl)pyrrolidine-2-carboxylic acid

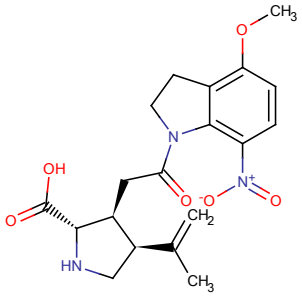

Prepared via a seven step synthesis from (2*S*,3*S*,4*S*)-kainic acid which in turn was obtained via in-house extraction from *Digenea simplex*.
^{1}H NMR (300 MHz) d_6-DMSO, δ 9.10 (v. broad, ex, 1H), 7.70 (d, 1H), 6.95 (d, 1H), 4.95 (s, 1H), 4.75 (s, 1H), 4.10 (m, 2H), 3.90 (s, 3H), 3.60 (d, 1H), 3.45 (m, 1H), 3.20 (m, 1H), 3.00 (m, 3H), 2.80 (m, 1H), 2.60 (dd, 1H), 2.40 (dd, 1H), 1.70 (s, 3H) (N.B. pyrrolidine NH not visible)
MS: ES^+ m/z 390.00 [M+H], 100%.
Anal. Calcd for $C_{19}H_{23}N_3O_6.1.0H_2O$: C, 56.01; H, 6.18; N, 10.31. Found: C, 55.94; H, 6.25; N, 10.22.
HPLC: >99%. Luna C18 3 µ 100 × 4.6 mm i.d. column. Column temp. = 25 °C, flow rate = 1 mL/min, detection wavelength 249 nm.
Gradient: 10-100% MeCN + TFA (0.1% v/v): TFA (0.1% v/v aq.) in 20 min. Held at 100% MeCN + TFA (0.1% v/v) for 10 min. t_R 7.81 min.
Isocratic: 23% MeCN + TFA (0.1% v/v): 77% TFA (0.1% v/v aq.) for 30 min. t_R 12.08 min.

MNI-caged NMDA

(2*R*)-4-(4-methoxy-7-nitro-2,3-dihydro-1*H*-indol-1-yl)-2-(methylamino)-4-oxobutanoic acid

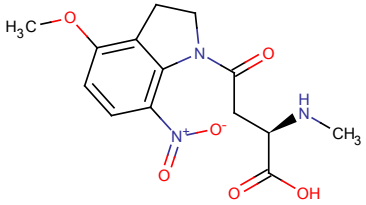

Prepared via a five step synthesis from a protected NMDA derivative.

^{1}H NMR (300 MHz) d_6-DMSO, ⌴ 7.80 (d, 1H), 6.90 (d, 1H), 4.30 (m, 2H), 3.95 (s, 3H), 3.55 (m, 1H), 3.15 (dd, 1H), 3.05 (m, 2H), 2.90 (dd, 1H), 2.55 (d, 3H) (N.B. carboxylic acid and NH not visible)
^{13}C NMR (75 MHz) d_6-DMSO, ⌴ 169.34, 167.92, 158.58, 135.94, 134.65, 124.84, 123.09, 107.21, 58.97, 56.15, 49.69, 35.03, 31.81, 25.84
MS: ES$^+$ 324.00 [M+H], 100%.
Anal. Calcd for $C_{14}H_{17}N_3O_6.0.5H_2O$: C, 50.60; H, 5.46; N, 12.64. Found: C, 50.38; H, 5.42; N, 12.34.
HPLC: >99%. Luna C18 3 µ 100 × 4.6 mm i.d. column. Column temp. = 25 °C, flow rate = 1 mL/min, detection wavelength 248 nm.
Gradient: 10-100% MeCN : ammonium acetate (50 mM, pH 8.0) in 20 min. Held at 100% MeCN for 10 min. t_R 5.25 min.
Isocratic: 12.5% MeCN : 87.5% ammonium acetate (50 mM, pH 8.0) for 30 min. t_R 9.85 min.
$[\alpha]_D$ = -16.8 (Concentration = 0.44, solvent = water, temp =23.3°C)

Because of concern about possible chiral instability of the NMDA moiety, the synthesis was repeated with racemic *N*-methylaspartic acid and the product was analysed by chiral HPLC. The results (see below) show that the MNI-caged NMDA retained its full chiral identity.
Chiral HPLC: Chiralpak QD-AX 5µ 150 x 4.6 mm i.d. column. Column temp = 15 °C, flow rate = 0.5 mL/min, detection wavelength 248 nm. Mobile phase: methanol : formic acid : ammonium hydroxide (100 : 1.5 : 1.0, v/v/v). The racemic material showed two peaks with t_R 8.24 and 9.74 min. MNI-caged NMDA showed a single peak, coincident with the later-eluting isomer, and corresponding to >99% e.e.

References:

Corrie, J.E.T., De Santis, A., Katayama, Y., Khodakhah, K., Messenger, J.B., Ogden, D., Trentham, D., 1993. Post-synaptic activation at the squid giant synapse by flash photolytic release of glutamate from a "caged" L-glutamate. J. Physiol. 465, 1-8.

Papageorgiou, G., Corrie,J.E.T., 2000. Effects of aromatic substitution on the photocleavage of 1-acyl-7-nitroindolines. Tetrahedron 56, 8197-8205.

Papageorgiou, G., Corrie, J.E.T., 2002. Regioselective nitration of 1-acyl-4-methoxyindolines leads to efficient synthesis of a photolabile L-glutamate precursor. Synth. Commun. 32, 1571-1577.

Papageorgiou, G., Ogden, D., Corrie, J.E.T., 2004. An antenna-sensitized nitroindoline precursor to enable photorelease of L-glutamate in high concentrations. J. Org. Chem. 69, 7228-7233.